

Principles of superfluid-helium gyroscopes

Richard E. Packard

Department of Physics, University of California, Berkeley, California 94720

Stefano Vitale

University of Trento and Istituto Nazionale di Fisica Nucleare, I-38050 Povo, Trento, Italy

(Received 16 September 1991; revised manuscript received 16 April 1992)

In this paper we describe how quantum coherence of superfluid helium provides a mechanism by which very small rotations can substantially modify the flow in a toroidal container. The specific modifications to that flow are discussed. For ^4He , we explain how the rotationally induced flow can be detected by monitoring the apparent phase-slip critical current. The rotational resolution is limited by stochastic processes related to the nucleation of phase slips. This type of superfluid-helium gyroscope (SHEG) is an analog of the rf superconducting quantum interference device (SQUID). We also show how the large coherence length of ^3He can be utilized to lead to a rotationally induced interference pattern. Changes in this pattern can permit the detection of very small rotational motion. This type of SHEG is analogous to the dc SQUID. In appendixes, electrical circuits equivalent to the SHEG are described, as are certain constraints on rotational sensitivity imposed by external measuring devices.

INTRODUCTION

This paper will describe the principles of devices, using superfluid helium, that will detect very small changes in the state of absolute rotation of the container holding the helium. It is possible that the sensitivity of this class of detector may eventually surpass existing gyroscope technology. Although a working superfluid gyroscope has not yet been demonstrated in the laboratory, the principles underlying its operation have been well established for many years and it seems likely that a working model will emerge in the near future.

Although some of the ideas underlying this potential technology have been recognized previously in various forms,¹⁻⁶ there has not yet been a consistent description of a possible practical device. It is the purpose of this paper to fill this void. We hope to present the basic principles of superfluid-helium gyroscopes (SHEG's) as they are presently understood. However, because this field is in its infancy, there are still many unanswered questions. Wherever possible, we point out those aspects of the problem which will require fundamental research.

Although the helium rotation sensors bear a close analogy to the superconducting quantum interference device (SQUID), both rf and dc, we have chosen to write this paper assuming the reader has no great familiarity with these devices. We have also not assumed any special knowledge of superfluidity.

A general discussion of the sensitivity of rotation sensors or of the uses of such sensors is beyond the scope of this paper. However, because there is already interest within the geodesy community in measuring very small changes in the Earth's rotation vector⁷ and also in the possibility of detecting the general-relativistic gravitomagnetic field⁸ of the Earth, we will tend to direct numerical estimates toward the greatest achievable levels of

sensitivity.

The paper is arranged as follows: After first describing the fundamental ideas behind these devices, we describe the nature of intrinsic dissipation critical velocities in superfluid ^4He , a topic intimately related to the practical realization of the gyroscope. We proceed to discuss a specific realization using ^4He . This is followed by a description of a device relying on ^3He and its specific properties when confined to a very small hole. In each case we present a discussion of the fundamental limitations of such devices. Following the main text, there are two appendixes. The first explains the electrical equivalent circuit of the SHEG. The second describes the nonintrinsic noise sources which might limit the sensitivity of the SHEG.

Whenever numerical estimates are made within this paper, we will use parameters that do not exceed current state of technology.

GENERAL PRINCIPLES

Both stable isotopes of helium (^3He and ^4He) undergo superfluid phase transitions at low temperatures (2.7 mK for ^3He and 2.17 K for ^4He). Below the transition temperature these liquids can exhibit flow without any dissipation.^{9,10} Superfluid systems are characterized by a macroscopic quantum-mechanical wave function $\Psi = \Psi_0 e^{i\phi}$, whose complex phase ϕ contains the kinematic description of the system and whose amplitude Ψ_0 is proportional to the superfluid density. Usually (in the case of ^4He and $^3\text{He-B}$), the gradient of the phase is related to the superfluid velocity field v_s by

$$\text{grad}\phi = (2\pi m / h) v_s, \quad (1)$$

where h is Planck's constant and m equals either the bare ^4He atomic mass or twice the atomic mass of ^3He . (The

factor of 2 comes from the fact that Cooper pairing underlies the ^3He superfluid state.) The ratio h/m will henceforth be designated by the symbol κ .

The relationship between macroscopic quantum phase and velocity, expressed by Eq. (1), leads to a restriction on the flow states accessible to a quantum liquid. To assure the single valuedness of the wave function, one must assume that, if the function $\text{grad}\phi$ is integrated around any closed path lying in the fluid, the total phase change must be an integral multiple of 2π . Thus

$$\oint \text{grad}\phi \cdot d\mathbf{l} = 2\pi n . \quad (2)$$

Combining this result with Eq. (1) leads to the flow-restriction condition

$$\oint \mathbf{v} \cdot d\mathbf{l} = nh/m = n\kappa , \quad (3)$$

which states that the fluid circulation is quantized around all paths lying within the fluid. The quantum of circulation, κ , has the values 0.99×10^{-7} and 0.66×10^{-7} m^2/s for ^4He and ^3He , respectively. Equation (3) has been experimentally verified^{11,12} in both ^3He and ^4He .

Now consider an annular container of mean radius R (see Fig. 1) and small cross section σ , filled with superfluid and partitioned at one place by a very thin wall. If this container is at rest, the superfluid ground state must have zero velocity, and it follows from Eq. (1) that the phase ϕ is constant throughout the liquid. However, if the vessel is rotated about a central axis (perpendicular to the plane of the annulus) at regular velocity Ω , the fluid must exist in a nonzero velocity state. The corresponding phase gradient given by Eq. (1) implies that a phase difference $\delta = \phi_2 - \phi_1$ will exist across the wall. We will show that a very small rotation rate can create a very substantial phase difference. If that phase difference can be measured, one can determine the state of absolute rotation of the annulus. Such phase differences *can* be measured, and this is the basic principle underlying this class of rotation sensor.

If the lateral dimensions of the torus are small compared with R , the velocity induced by rotation must be close to the solid-body value¹³ $v = \Omega R$. In this case the phase difference is given by

$$\delta = \int_1^2 \text{grad}\phi \cdot d\mathbf{l} = \frac{4\pi^2 \Omega R^2}{\kappa} . \quad (4)$$

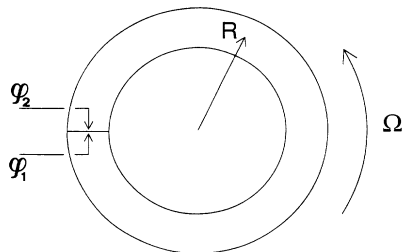


FIG. 1. Rotating annular container partitioned by a thin wall.

Because all physical observables related to the wall are periodic in δ , the greatest physically distinguishable phase difference across the partition is $\delta = \pi$. The angular velocity which produces this maximum phase difference is given from Eq. (4) by setting $\delta = \pi$:

$$\Omega_\pi = \kappa / 4\pi R^2 . \quad (5)$$

For the case of ^4He , if $R = 0.5$ m, $\Omega_\pi = 3 \times 10^{-8}$ rad/s = $4 \times 10^{-4} \Omega_E$. Here Ω_E is the Earth's daily rotation rate and is, for geodetic purposes, a useful unit of angular velocity. (It should be mentioned that a device of 1 m lateral dimension seems like the largest feasible device. This scale matches the technology which is presently in use for cryogenic gravity-wave detectors.¹⁴ Clearly, small angular velocities can produce appreciable phase differences for scale lengths achievable in a laboratory setting.

For an N -turn torus or radius R , the phase difference for a given Ω will be N times greater than that given by Eq. (4). However, as shown below, there is a practical limit for the maximum number of toroidal turns.

If one uses a technique to measure phase differences across a partition, it should be possible to create a sensitive sensor of absolute rotation.

The next sections describe possible techniques for detecting these rotationally induced phase differences in ^4He and ^3He .

ROTATIONALLY INDUCED FLOW THROUGH AN ORIFICE

To probe the phase difference of Eq. (4), we may place a very small hole, of radius r , in the thin partition. A given phase difference across the small length of the partition implies a very large phase gradient and, through Eq. (1), a velocity in the hole which is very large compared to ΩR .

Consider the torus initially at rest with the fluid in the zero-circulation state. If the torus begins to rotate slowly, the circulation will not change. This implies that, in the circulation integral, the term arising from the solid-body flow in the torus must be balanced by a counterflow in the orifice. The superfluid gyroscopes described in this paper involve methods of detecting the rotationally induced velocity field in the orifice.

The size of the rotation-induced flow velocity in the hole, v_Ω , can be estimated by using the quantization of the circulation condition. In the rotating torus we let the velocity far from the orifice, as seen in the nonrotating frame, be $v = \Omega R$. The effective length of the orifice, l_{eff} , can be obtained by solving the potential flow problem for a round hole in a thin partition and then equating the total kinetic energy to $\frac{1}{2} \rho \pi r^2 l_{\text{eff}} v^2$. Here the velocity v is the mean velocity defined by the ratio of volume flow rate to orifice area. The effective length is found to be¹⁵ $l_{\text{eff}} = \pi r / 2$, so that $\delta = v l_{\text{eff}} / \kappa$.

Performing the circulation integral then gives the equation

$$2\pi R \Omega R + \frac{v_\Omega \pi r}{2} = n\kappa . \quad (6)$$

Solving for v_Ω , the velocity induced in the orifice, gives

$$v_\Omega = (2/\pi r) \{ n\kappa - 2\pi R^2 \Omega \} . \quad (7)$$

Perhaps the most intuitive way to view this equation is to point out that, for the zero-circulation state ($n=0$), the rotation-induced fluid velocity in the hole is greater than the linear velocity of the torus (ΩR) by the large factor $4R/r$. For example, if $R=0.5$ m and $r=0.5 \times 10^{-6}$ m, the fluid velocity in the orifice exceeds the tangential speed of the torus by 4×10^6 .

The discussion leading to Eq. (7) has ignored the modification of the flow in the body of the torus caused by the presence of the hole. A more complete derivation (see Ref. 2 and Appendix A) of Eq. (7), for the case of an N -turn torus, yields the result

$$v_\Omega = \frac{2}{\pi r} \frac{n\kappa - 2\pi NR^2 \Omega \cos\theta}{1 + 4\pi NRr/\sigma} , \quad (8)$$

where θ is the angle between the rotation vector and the normal to the plane of the torus and σ is the torus cross-sectional area.

Notice that v_Ω is evaluated in a reference frame rotating with the torus. In the inertial frame one should add the negligibly small velocity ΩR .

The quantity $2\pi NR^2 \Omega \cos\theta$ is the flux of the vector 2Ω through the torus. For simplicity in this paper we will assume that $\theta=0$. By making the electrical analog (see Appendix A) for a fluid flowing through a tube of length l and area σ , one can introduce the concept of the kinetic inductance $L=l/\rho\sigma$. Inspection of Eq. (8) shows that the denominator term is a correction to Eq. (7), which involves the ratio of the inductance of the N -turn torus to that of the orifice.

Equation (8) is, for a superfluid such as ^4He , the fundamental gyroscope equation. We will now discuss the physical phenomenon through which one may measure the fluid velocity in a small hole and thus detect the rotationally induced flow described above.

THE CRITICAL VELOCITY AND THE DETECTION OF THE ROTATIONALLY INDUCED FLOW

It has been known for many years that dissipation-free superflow will not exist for arbitrarily large fluid velocities.¹⁶ Over the past half century, there have been many measurements and several theories to describe the breakdown of superflow at a well-specified critical velocity. Of concern to us here is the intrinsic dissipation processes that occur in a submicrometer orifice at temperatures low enough so that normal-component flow is of no consequence.

The important relevant concept is that of the phase slippage as proposed by Anderson.¹⁷ He showed that, when the flow through the orifice attains some critical value, a quantized vortex line may be created which will move across the orifice, crossing all streamlines of the potential flow. It can be shown that in such a process the phase difference δ across the orifice will change by 2π and the flow energy will be reduced by $\Delta E = \kappa\rho s v_c$, where v_c is the critical velocity in the hole whose area is s .

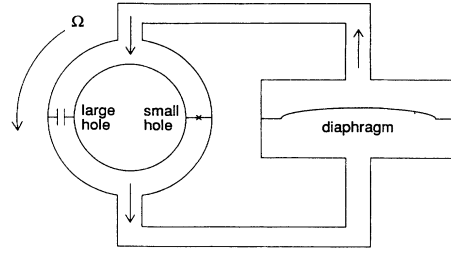


FIG. 2. Rotating partitioned torus, coupled to a diaphragm mass-current pump. Voltages applied to electrodes placed near the metallized diaphragm can induce the current.

Direct detection of individual 2π -phase-slip events has been reported by Avenel and Varoquaux (AV).¹⁸ The fundamental 2π phase slips have also been studied recently by us.¹⁹

Consider a rotating torus partitioned on one side by a thin wall which contains a submicrometer orifice. Suppose an external mass current I is driven through the torus. Figure 2 illustrates one particular configuration, which includes a mass-current source with the torus. With proper choice of the size of the torus and orifice, the mass current will split between the two arms, so that a substantial part of the mass flow will cross the orifice. Namely, this is obtained (see Appendix A) if the kinetic inductance of the half torus opposite to the orifice, $L_2=l_2/\rho s_2$ with l_2 the length of the arm and s_2 its section, is comparable to that of the torus other arm, $L_1=l_1/\rho s_1 + l_{\text{eff}}/\rho\pi r^2$. Here the second term $L_0=l_{\text{eff}}/\rho\pi r^2$ is the contribution due to the orifice.

Suppose now that the value of driven current I_c at which phase slip occur is recorded (see the discussion below). The flow in the orifice contains contributions both from the external drive and from rotationally induced flow, given by Eq. (8). Since the critical velocity for a given orifice (at fixed temperature) has a fixed value, the rotation will produce a shift in I_c . This shift is identical to that caused by an apparent change in critical velocity to $v_c \pm v_\Omega$, the sign depending on the sense of rotation. The shift in I_c is the basic observable which determines the rotation rate.

LIMITS OF SENSITIVITY

In Eq. (8) is differentiated with respect to angular velocity, we can compute a rotation sensitivity G for a superfluid gyroscope. Thus

$$G = \left| \frac{d\Omega}{dv_\Omega} \right| = \frac{r \{ 1 + 4\pi NRr/\sigma \}}{4NR^2} . \quad (9)$$

A very small value of G implies a very sensitive sensor.²⁰

For a practical device of greatest sensitivity, one would typically select the torus radius R to fit the largest available cryostat and then make the number of turns, N , large enough so that the factor G was almost independent of N . If N is increased so that $4\pi NRr/\sigma = L_t/L_0 = 1$,

there is little to be gained from a further increase in N . Here L_t is the kinetic inductance of the torus, $L_t = L_1 + L_2 - L_0$. Thus, in computing the optimal practical sensitivity, we will let N take the value satisfying this latter equation. This yields the best rotation sensitivity for a given size apparatus. For this value of N , Eq. (9) gives

$$G_{\min} = \frac{2\pi r^2}{\sigma R}. \quad (10)$$

One can show that, for an orifice which is not circular, the numerator in the above expression has to be replaced by the twice the orifice area.

If we assume that the variations in angular velocity are detected through apparent variations in a measured critical velocity, then the minimum detectable angular velocity change is simply the product of G and the minimum detectable change in critical velocity, $(\delta v_c)_{\min}$:

$$(\delta\Omega)_{\min} = G(\delta v_c)_{\min}. \quad (11)$$

The discussion of the minimum detectable change in the critical velocity contains several different aspects. Perhaps the most fundamental issue is the question of how precise one could determine v_c if all other sources of instrumental noise were negligible. (In Appendix B we discuss the limits set by external instrumental noise.)

Although critical velocities in submicrometer orifices have been observed in many laboratories, no one as yet fully understands the dynamics of the phase-slip processes. However, from the observed temperature dependence of v_c , Varoquaux, Zimmermann, and Avenel²¹ have constructed a model involving thermally activated vortices created near the walls of an orifice. Their calculation predicts a thermal width Δv_c for the distribution of observed critical velocities given by

$$\Delta v_c = \frac{2v_{c0}k_B T}{E_0 \ln 2}, \quad (12)$$

where v_{c0} and E_0 are constants. Their experiments provide the empirical values $E_0/k_B = 106$ K and $v_{c0} = 10$ m/s. It is very important to note that, in the data of Ref. 21, the linear temperature dependence suggested by Eq. (12) is seen on top of a temperature-independent offset. If the observed offset is caused by disturbances, which can be eliminated by vibration isolation or other means, then Eq. (12) indicates that, if one measures the critical velocity many times in the same orifice, one will see a distribution of values of width 0.27 m/s at $T = 1$ K or, if the behavior can be extrapolated down there, 2.7×10^{-3} m/s at 10 mK.²² If the critical velocity is measured M times, the minimum detectable change will be

$$(\delta v_c)_{\min} = \frac{\Delta v_c}{\sqrt{M}}. \quad (13)$$

If one repeats the measurements at a rate f for a time τ so that $M = f\tau$, then

$$(\delta v_c)_{\min} = \frac{\Delta v_c}{\sqrt{f\tau}}. \quad (14)$$

Combining Eqs. (10)–(12) and (14) gives the rotation sensitivity

$$(\delta\Omega)_{\min} = \frac{2\pi r^2}{\sigma R} 2v_{c0}k_B T / E_0 \ln 2 \frac{1}{\sqrt{f\tau}}. \quad (15)$$

For an estimate we take $r = 0.5 \times 10^6$ m, $R = 0.5$ m, $\sigma = 10^{-4}$ m², and $T = 10$ mK. To optimize the sensitivity these parameters require 32 turns in the torus. Then Eq. (15) predicts a minimum detectable $\delta\Omega$ of about $1 \times 10^{-6} \Omega_E / (f\tau)^{1/2}$. If the observed temperature-independent offset²¹ of Δv_c is intrinsic to the phase-slip process, then at 10 mK the attainable sensitivity might be about a factor of 30 worse than indicated by Eq. (15). For a more modest parameter set of $R = 0.1$ m, $\sigma = 10^{-5}$ m², $T = 1$ K, and $r = 0.5 \times 10^{-6}$ m, one requires 16 turns and the detectable rotation is $6 \times 10^{-3} \Omega_E / (f\tau)^{1/2}$.

It appears from the above discussion that, for a given physical size of the torus, the important parameter to increase the sensitivity of the gyroscope is the measurement frequency f . (However, see Appendix B.) It may be possible that phase slips can be produced by mechanisms leading to a smaller value of the intrinsic width Δv_c . For instance, it may be possible to inject quantized vortex rings into the orifice, which would then serve as nucleation centers for the phase slips.

Mechanical vibrations of the apparatus are likely to play a twofold role: Vibrations ending in a solid-body rotation of the apparatus will act as any other rotation input to the sensor and cannot be discriminated from signals. On the other hand, mechanical noise can induce random flow nearby the orifice that will increase the width Δv_c above the thermal level discussed above. Note, however, that it is unlikely that the temperature-dependent offset, observed experimentally²¹ in the only measurement of Δv_c , is due to mechanical vibrations²³ and it may be due to intrinsic processes which cannot be eliminated. Future research is clearly needed to determine the minimum achievable value of Δv_c .

GYROSCOPE USING A HELMHOLTZ OSCILLATOR

Recent attention has been focused on the behavior of a superfluid oscillator described by Zimmermann and co-workers²⁴ and used successfully by Avenel and Varoquaux¹⁸ to detect single 2π -phase-slip events.¹⁸ In this section we explain how this device can be configured to detect the apparent change in v_c induced by rotation.

The Zimmermann-Avenel-Varoquaux (ZAV) oscillator, configured as a rotation sensor, is essentially the device shown in Fig. 2. The system described has a characteristic resonant mode arising from the spring constant of the diaphragm and the fluid inertia in the two holes. At low temperatures, where the normal fraction is negligible, or by assuming this fraction to be immobilized by some porous media, the frequency is given by

$$\omega_0^2 = \frac{k}{\rho S^2} \left[\frac{1}{L_1} + \frac{1}{L_2} \right], \quad (16)$$

where ρ is the total fluid density, ρ_s/ρ is the superfluid fraction, k is the spring constant of the diaphragm, S is

the diaphragm's effective area, and L_1 and L_2 are the kinetic inductances of the two arms of the torus as defined in the previous section.

The system somewhat resembles the classic Helmholtz resonance exemplified by a bottle with constricted neck. Because of this similarity (weak though it may be), the superfluid oscillator shown above has been frequently called a "Helmholtz oscillator."

The diaphragm can be electrically manipulated and the resonance excited by the application of a voltage to a fixed metal plate located nearby. If the diaphragm is coated with a superconducting film, it can serve as the movable element in a sensitive superconducting displacement transducer.

Analysis of the fluid flow permits one to derive a relation between the velocity in the small hole, v_h , and the velocity of the diaphragm, V_d . This last quantity is defined such that $\rho S V_d$ is the mass flow displaced by the diaphragm. The result, when there are no trapped circulation quanta, is

$$V_d = \frac{\pi r^2}{S} (1+B)(v_h + v_\Omega), \quad (17)$$

where $B = L_1/L_2$, πr^2 , as above, is the area of the orifice, S is the diaphragm area, and v_Ω is given by Eq. (8) above. In Eq. (17) the directions of the velocities are chosen such that a positive V_d will produce, in the absence of trapped quanta and for $\Omega=0$, a positive v_h .

If the oscillator is driven by a resonant applied force, the velocity amplitude of the diaphragm may increase until the hole velocity v_h reaches the critical velocity v_c for a phase slip. At this point in the phase across the hole slips by 2π , removing energy from the oscillator and injecting one quantum of circulation in the torus. The energy decrement causes the oscillation amplitude to abruptly drop. Because of the additional current caused by the added circulation, usually the phase will slip again in the next half cycle. Unless the applied force increases substantially, the oscillator amplitude cannot rise above the critical amplitude A_c , which corresponds to the velocity in the hole reaching v_c . By measuring the diaphragm's critical oscillation amplitude A_c when the phase slip occurs, one can determine the value of the diaphragm's velocity $V_{dc} = \omega_0 A_c$ when $|v_h| = v_c$. From Eqs. (17) and (8) it follows that

$$A_c = (v_c + v_\Omega) \frac{\pi r^2 (1+B)}{S \omega_0} = \left[v_c + \frac{(2/\pi r)(n\kappa - 2\pi N R^2 \Omega)}{1 + 4\pi N R r / \sigma} \right] \frac{\pi r^2}{\omega_0 S} (1+B). \quad (18)$$

If the rate of rotation changes, there is a corresponding change in A_c ,

$$\left| \frac{\delta \Omega}{\delta A_c} \right| = \frac{\omega_0 S}{R \sigma}. \quad (19)$$

The changes in flow in the orifice are a factor $S/\pi r^2$ times greater than the corresponding changes in the diaphragm velocity. Thus, again, in analogy with Eqs. (10)

and (11), we get, for the smallest detectable change in angular velocity,

$$(\delta \Omega)_{\min} = \frac{\pi r^2}{\sigma R} (\delta v_c)_{\min}, \quad (20)$$

where $(\delta v_c)_{\min}$ is given by Eq. (14). This result is essentially that of Eq. (15) except that, since the critical amplitude can be measured at most twice in one oscillator cycle, the measuring frequency entering Eq. (15) must be that of the oscillator itself, $f_0 = \omega_0/2\pi$. Thus, for the ZAV oscillator, the minimum detectable change in angular velocity is

$$(\delta \Omega)_{\min} = \frac{\pi r^2}{\sigma R} \frac{\Delta v_c}{\sqrt{f_0 \tau}}. \quad (21)$$

A more complete analysis⁶ of the ZAV oscillator reveals that the variation of oscillation amplitude with driving force exhibits a staircase pattern. The diaphragm amplitude in Eq. (18) is that for the first step. The change in the critical diaphragm amplitude between two adjacent steps is the same as the change in A_c caused by a rotation that produces a 2π phase shift across the orifice.

If the critical amplitude of one step is plotted as a function of rotation rate Ω , a characteristic triangle pattern will be produced.²⁵ The periodicity of the pattern is the quantum of rotation flux κ . If the flux of 2Ω , $2\Omega N \pi R^2$, increases by κ , the triangle pattern passes through one complete cycle.

It is not yet known what the upper limit of the Helmholtz frequency can be. The only successful device (i.e., showing a staircase pattern) yet demonstrated²⁶ had a characteristic frequency of only a few Hz. Furthermore, attempts to see the staircase pattern using higher-frequency oscillators were unsuccessful,^{2,27,28} although this may have been due to problems with the orifice or due to too high a temperature.

To create the staircase pattern, the transient, due to a single phase slip, must decay within the torus in a time less than one-half of a cycle of oscillation. On steps higher than the first one, where multiple phase slips take place, the decay should even be faster. This relaxation process is not understood at present, but it may involve acoustic dissipation, which is typically very slow in superfluids. At this point it is not known what physical process will limit the maximum frequency in the ZAV oscillator.

Possibly an upper frequency limit is determined by the time $\approx r/v_c$ it takes a vortex line to cross the orifice. This limiting frequency is about 10^5 Hz for an orifice with diameter 10^{-6} m. In this limit a SHEG based on the ZAV oscillator would be of use both in geodetics⁷ and gravitomagnetics.⁸

It is important to make clear that, at this writing, only Avenel and Varoquaux have succeeded in achieving the conditions to create the staircase pattern. It is not yet clear what the important parameters are to create an oscillator which exhibits this characteristic. Clearly, several important questions must be answered in future research.

GYROSCOPE USING QUANTUM INTERFERENCE

Although ^3He exists as a superfluid (below 2×10^{-3} K), the physics involved in a flow through a small orifice is very different from that discussed above for ^4He . The most significant difference involves the magnitude of a length ξ , which characterizes the distance over which the wave function amplitude can have significant variations. This so-called coherence length is of the order of 0.1 nm in ^4He , but in ^3He is almost three orders of magnitude larger. For the case of ^3He , one finds⁹

$$\xi = \frac{\xi_0}{\sqrt{1 - T/T_c}}, \quad (22)$$

where T_c is the superfluid transition temperature and ξ_0 , the zero-temperature coherence length, is about 70 nm at low pressures.

If a superfluid is confined to a space whose dimensions are on the order of ξ , the wave function becomes quite modified and, for flow, the linear current-phase relation implicit in Eq. (1) is no longer valid. For ^4He in an orifice with dimensions > 100 nm, the very short coherence length assures the applicability of Eq. (1). However, for the case of ^3He in an orifice whose size is comparable to ξ , there is experimental evidence²⁶ and theoretical reason²⁹ to believe that the current-phase relation is given by the dc Josephson relation

$$I = I_c \sin \delta. \quad (23)$$

In their experiments on phase-slip phenomena, Avenel and Varoquaux showed²⁶ that, in ^3He , as the size of ξ increased, the current-phase relation changed continuously from linear ^4He -like behavior to that characterized by Eq. (23).

In the discussion which follows, we will assume that Eq. (23) is a good approximation for an orifice in a partition whose thickness and at least one lateral dimension are comparable to ξ . Thus the apertures of interest must exist in a wall of thickness ≈ 100 nm and must have at least one other dimension of comparable size. The manufacture of such elements is well within the current microfabrication technology.³⁰ Figure 3 shows the basic

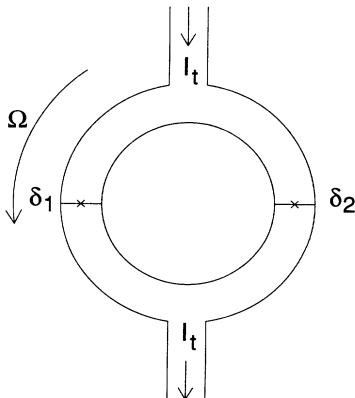


FIG. 3. ^3He Josephson interferometer.

topology of a ^3He gyroscope based on quantum interference. The torus contains similar small orifices in each side. We will calculate the maximum supercurrent through the device as a function of rotation rate.

For algebraic simplicity we will assume that the weak links are identical. A current I_t is injected into the torus by the motion of a diaphragm pump (such as that shown in Fig. 2). In the torus reference frame, I_t divides, with current I_1 passing through the right-hand branch and current I_2 passing through the left-hand side. The mass currents in the two sides as viewed in the inertial frame are

$$I_1^* = I_1 + \Omega R \rho \sigma \quad \text{and} \quad I_2^* = I_2 - \Omega R \rho \sigma, \quad (24)$$

where, as before, σ is the cross-sectional area of the torus and R is the radius. The sum of the currents is always equal to I_t , independent of the frame of reference. The sinusoidal current-phase relation holds in the frame of the orifice, i.e., the rotating frame.¹ Thus

$$I_1 = I_c \sin \delta_1 \quad \text{and} \quad I_2 = I_c \sin \delta_2, \quad (25)$$

where, as before, we are letting δ symbolize the phase difference across the orifice.

If the two equations in (25) are added, we get

$$\begin{aligned} I_t &= I_c \sin \delta_1 + I_c \sin \delta_2 \\ &= 2I_c \sin \left[\frac{\delta_1 + \delta_2}{2} \right] \cos \left[\frac{\delta_1 - \delta_2}{2} \right]. \end{aligned} \quad (26)$$

We can find an expression for the difference term by using the restriction of Eq. (2), which holds in the inertial frame. This gives

$$\begin{aligned} \delta_1 - \delta_2 &= \frac{2\pi R}{\rho \kappa \sigma} (I_2 - I_1) - \frac{4\pi^2 \Omega R^2}{\kappa} \\ &= \frac{2\pi R_s}{\sigma \kappa} (v_2 - v_1) - \frac{4\pi^2 \Omega R^2}{\kappa}, \end{aligned} \quad (27)$$

where, in the second line, we have written the currents in the orifices in terms of the average fluid velocity, with respect to the orifice. The symbol s represents the area of a single orifice. Because the currents depend on δ through the dc Josephson relation, Eq. (27) is nonlinear. However, the typical critical velocity in ^3He is on the order of 10^{-2} m/s and the area s must typically be about 10^{-13} m². Then, for any reasonable value of R and σ , the first term on the right-hand side will always be much smaller than the second and will be ignored in what follows.

The phase differences in the two reference frames differ by only a very small amount (the Galilean boost term $\Omega R I_{\text{eff}} 2\pi/\kappa$) and may be taken to be identical. Combining Eqs. (26) and (27) gives

$$\begin{aligned} I_t &= 2I_c \cos \frac{2\pi^2 \Omega R^2}{\kappa} \sin \frac{\delta_1 + \delta_2}{2} \\ &= I_0 \sin \Delta, \end{aligned} \quad (28)$$

where

$$I_0 = 2I_c \cos \frac{2\pi^2 \Omega R^2}{\kappa} \quad (29)$$

is the maximum supercurrent that can flow through the device and $\Delta = (\delta_1 + \delta_2)/2$ is the phase difference across the entire device. Equation (29) implies that, as far as the diaphragm current is concerned, the entire rotating torus behaves like a single Josephson device whose critical current is modulated by the angular velocity. If the quantity $\pi R^2 2\Omega$ is thought of as the flux of the vector 2Ω , the modulation flux period is κ .

For a torus with N turns, Eq. (29) would be modified by the factor N multiplying the argument of the cosine term.³¹

Equation (29) is the important result for the ^3He gyroscope. It plays the same role as does Eq. (8) for the ^4He gyroscope. For an N -turn torus, changes in angular velocity are related to changes in maximum current through the relation

$$G = \frac{\delta\Omega}{\delta I_0} = - \frac{\kappa}{4I_c \pi^2 N R^2 \sin(2\pi^2 N R^2 \Omega / \kappa)} \quad (30)$$

The best sensitivity as a rotation sensor is achieved if the device is "biased" so that the sinusoid in the denominator is near unity.

In a physical realization of the ^3He rotation sensor, the current I_c would be supplied from the motion of a diaphragm, similar to the arrangement shown in Fig. 2. If a stepwise dc potential is applied to a fixed electrode near the diaphragm, a pressure head ΔP will appear across the torus and the diaphragm will move toward the electrode at an almost constant velocity, determined by the maximum mass current I_0 . The motion of the diaphragm is monitored by a sensitive displacement transducer (see Appendix B).

The minimum detectable variation in Ω is given by the product of G and the minimum detectable variation in current through the device:

$$(\delta\Omega)_{\min} = |G| (\delta I_0)_{\min} \quad (31)$$

There must be some intrinsic thermal limit on δI_0 , but it is not obvious exactly what to assume this limit to be. However, we may be guided by the close analogy between this dc SHEG and the closely analogous dc SQUID.³² In the latter device the intrinsic limit is related to thermal noise arising in a parallel resistive element. There is no apparent similar element for the dc SHEG, except perhaps for the leakage through the orifice due to ballistic quasiparticles driven by the pressure head.

The characteristic energy barrier that prevents phase uncoupling of the superfluid on two sides of the Josephson junction is given by $E_1 = \kappa I_c / 2\pi$. It would seem that the fractional width of the distribution function characterizing the phase unwinding must be at least as big as kT/E_1 , which is on the order of 10^{-4} for ^3He . If we multiply G by $10^{-4} I_c$, we obtain a thermal limit for smallest detectable change in Ω .

To make an optimistic numerical estimate of the sensitivity factor G , one might take values for the case $R = 0.1$

m, $N = 1$. This suggests a value of $(\delta\Omega)_{\min} = 2 \times 10^{-7} \Omega_E / \sqrt{\tau f_{JA}}$. The frequency of operation is presumably the Josephson-Anderson frequency¹⁷ $f_{JA} = \Delta P / \kappa \rho$, where ΔP is the pressure head across the torus. However, the quantum interference phenomenon, leading to Eq. (29), will break down on time scales shorter than some characteristic relaxation time in the torus. As in the case of the ^4He SHEG, these relaxation processes are not yet understood and are the subject of ongoing research.

The estimate above may be overly optimistic because of our present inadequate state of knowledge concerning the role of intrinsic noise processes for this device. It should also be emphasized that there are additional noise contributions arising from thermal motion of the diaphragm and limitations in the SQUID displacement transducer. These are discussed in Appendix B.

It appears that the rotation sensor described in this section offers a greater possible sensitivity than that described for ^4He . Aside from the different transfer functions for the two types of devices, the dc SHEG must have the advantage that, for a given pressure drive ΔP , the phase is "slipping" at the Josephson-Anderson frequency $f_{JA} = \Delta P / \rho \kappa$. A typical value of ΔP might be about 1 Pa, giving a frequency near 10^5 Hz. Ultimately, this high sampling rate must win out over the much lower-frequency ZAV oscillator.

CONCLUSION

We have described the basic principles of rotation sensors exploiting quantum phase shifts in superfluid helium. One device, using ^4He , depends on the critical velocity at which vortices are generated in a small orifice. Another device uses ^3He and exploits the nonlinear relationship between current and phase, which is appropriate for orifices about 100 nm in dimension.

There are still many significant questions that need to be answered to understand fully the limit of this emerging technology. Presently, perhaps the most pressing need is for a demonstration of the detection of small rotations by one of the two devices described herein. Such a demonstration will lead in a natural way to the answers of some of the important issues raised.

ACKNOWLEDGMENTS

It is a pleasure to acknowledge helpful and stimulating conversations with the following colleagues: O. Avenel, E. Varoquaux, W. Zimmermann, Jr., L. Pitaevskii, M. Cerdonio, M. Bonaldi, J. C. Davis, A. Amar, Y. Sasaki, K. LaRana, R. Chiao, and J. Anandan. We also thank the gracious hospitality of Istituto Bronzini. This work was partially supported by a joint contract from the U.S. Air Force Geophysical Laboratory, the National Oceanic and Atmospheric Administration, and the Institute Für Angewandte Geodasie. Preliminary aspects of this work were supported by a grant from the National Science Foundation.

APPENDIX A

The analysis of the SHEG can be cast in familiar electrical analogs if one considers an equivalent circuit for the device. The key ingredients in this analysis are the concept of kinetic inductance, the role of abrupt 2π phase slips, and the role of pressure driving terms.

Consider a tube of area s and length l through which fluid of mass density ρ flows at mean velocity v . The kinetic energy of the fluid in the tube is

$$K = \frac{1}{2} \rho v^2 s l. \quad (\text{A1})$$

This can be written in terms of the mass current $I = \rho v s$,

$$K = \frac{1}{2} \frac{1}{\rho s} I^2 = \frac{1}{2} L I^2, \quad (\text{A2})$$

where the $L = 1/\rho s$ is called the kinetic inductance of the tube. This quantity can also relate the time derivative of the mass current resulting from a driving pressure ΔP across the tube:

$$\frac{\Delta P}{\rho} = \frac{l}{\rho s} \frac{dI}{dt} = L \frac{dI}{dt}. \quad (\text{A3})$$

The driving term on the left is the chemical potential difference ΔV , and so the latter equation becomes

$$\Delta V = L \frac{dI}{dt}. \quad (\text{A4})$$

Equations (A2) and (A3) show that the kinetic inductance places the normal role of inductance in circuits.

A small orifice in the potential flow regime also obeys Eqs. (A3) and (A4), but with $L = 1/2\rho r = l_{\text{eff}}/\rho\pi r^2$.

In terms of inductance, the quantization of circulation condition, in a torus containing two distinct flow sections (e.g., a small hole and a large channel) appears as

$$L_1 I_1 + L_2 I_2 = n \kappa. \quad (\text{A5})$$

The effect of a 2π phase slip at time τ can be deduced by treating the phase-slip event as a generator of potential difference of the form

$$\Delta V_s = \pm \kappa \delta(t - \tau), \quad (\text{A6})$$

where the sign has to be chosen so that the pressure pulse tries to decrease the flow through the orifice. Thus a 2π phase slip, occurring in the torus consisting of two lumped inductances, creates a mass current $I_q = \pm \kappa / (L_1 + L_2)$.

A final useful result is that, for two kinetic inductances connected in parallel, an impressed pressure head would drive a total current $I_t = I_1 + I_2$ through the pair as if they were inductors in parallel. The total current through the parallel pair increases as

$$\frac{dI_t}{dt} = \left[\frac{1}{L_1} + \frac{1}{L_2} \right] \Delta V \quad (\text{A7})$$

and

$$I_1 = I_t \frac{L_2}{L_1 + L_2} \quad \text{and} \quad I_2 = I_t \frac{L_1}{L_1 + L_2}. \quad (\text{A8})$$

The motion of the diaphragm in Fig. 2 is described by the differential equation

$$m \frac{d^2 x}{dt^2} + \beta \frac{dx}{dt} + kx = F + S \Delta P, \quad (\text{A9})$$

where x is the diaphragm's effective displacement, m is its effective mass, k is its effective stiffness, and β is a damping coefficient. As in connection with Eq. (17), x is defined such that the total fluid mass displaced by the diaphragm per unit time is $I_t = S\rho dx/dt$, while the effective stiffness mass and damping coefficients are chosen such to give the proper free oscillation frequency and decay time.

The right-hand side of Eq. (A9) includes a driving force F , usually of electric origin in practical devices, and the force due to the pressure difference ΔP on the diaphragm's effective surface S . If we define an analog of "charge" as $Q_t = \rho S x$, so that $I_t = dQ_t/dt$ and express ΔP as $\Delta P = \rho \Delta V$, then Eq. (A9) can be recast as

$$L_d \frac{dI_t}{dt} + R I_t + \frac{Q_t}{C} + \Delta V_g = \Delta V, \quad (\text{A10})$$

with $L_d = m / (S\rho)^2$, $R = \beta / (S\rho)^2$, $1/C = k / (S\rho)^2$, and $\Delta V_g = -F / (S\rho)$. Equation (A10) is formally equivalent to that describing the voltage and current in a series circuit composed of an inductor L_d , a resistor R , a capacitor C , and a voltage generator ΔV_g . ΔV is then the total voltage drop across the circuit.

In the ZAV oscillator the current I_t displaced by the diaphragm divides between the two parallel kinetic inductances in the ratios implied by Eq. (A8). If the inductances of the tubes connecting the diaphragm to the torus are negligible, then the potential difference across the diaphragm is the same as that across the torus. The dynamics of the ZAV oscillator is then analogous to the circuit in Fig. 4.

From the electrical equivalent circuit of the ZAV oscillator and standard methods of circuit theory, one can

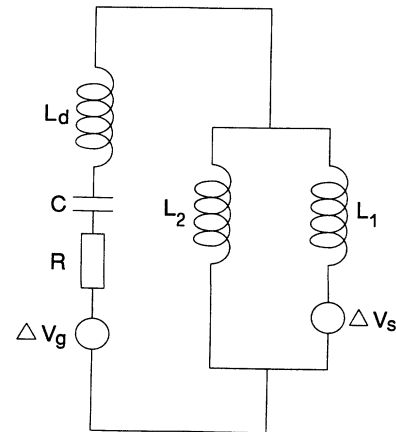


FIG. 4. Electrical equivalent circuit for the ZAV oscillator.

compute the dynamical effects of a 2π phase slip. Suppose that a constant amplitude oscillating drive $\Delta V_g = \Delta V_0 \cos(\omega_0 t)$ is applied at the oscillator resonance frequency $\omega_0 = (L_T C)^{-1/2}$ with $L_T = L_d + L_1 L_2 / (L_1 + L_2)$. The current in the orifice will oscillate with increasing amplitude until the critical current I_c in the orifice is reached.

If the drive amplitude is not too high, the critical current will be reached when the current oscillation is near one of its maxima or minima and the diaphragm displacement is correspondingly close to zero. The phase slip has two consequences: (i) The oscillation amplitude for the total current I_t drops by an amount $\Delta I_t = \kappa / L_1$. (ii) A steady current $I_q = \pm \kappa / (L_1 + L_2)$ circulates around the torus superimposed to the current due to the diaphragm motion.

The result of these two effects is that, after the phase slip, the current in the orifice is reduced by $\Delta I_1 = \kappa / L_1$, while that in the parallel channel does not change at all.

The total work done by the equivalent voltage generator (i.e., the work done by the phase-slip process) is found to be

$$W = -I_c \kappa + \kappa^2 / 2L_1. \quad (\text{A11})$$

This equals the decrease in the kinetic¹⁷ energy of the flow through the orifice.

The effect of rotation can be reformulated in term of the linear circuit of Fig. 4 expressing the quantization of circulation in term of the current circulating in the torus:

$$(L_1 + L_2)I_q + 2\pi N R^2 \Omega = n \kappa. \quad (\text{A12})$$

This is analogous to flux quantization in a superconducting ring if the quantity $2\pi N R^2 \Omega$ is taken as the external flux threading the ring and κ as the quantum of flux. If the velocity in the orifice corresponding to I_q is calculated, $v_\Omega = I_q / (\rho \pi r^2)$, Eq. (8) with $\theta = 0$ is then recovered.

A circuit analysis is also possible when the orifice behavior approaches the Josephson one. This is the case for ^3He when the coherence length approaches the dimensions of the orifice. In this case the equivalent circuit is similar to Fig. 4 except the voltage generator ΔV_s is replaced by a nonlinear element characterized by the current-phase relation $I = I_0 \sin \delta$. Though the circuit is no more linear, it is still suitable for approximated analysis or numerical simulation in close analogy with the resistively shunted junction³³ (RSJ) model for the SQUID.

APPENDIX B

Besides the intrinsic fluctuation of the critical current coming from the stochastic nature of the phase-slip processes, at least two other sources of noise can be identified in the ZAV oscillator: the noise of the transducer used to read diaphragm displacement and the thermal (Brownian) noise of the oscillator itself.

The position of the diaphragm is monitored by making it a part of an inductive motion transducer. The diaphragm is coated by a superconducting layer and is posi-

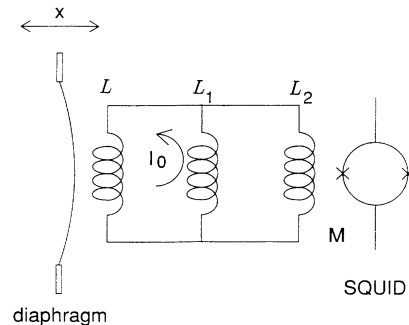


FIG. 5. Equivalent circuit for the motion transducer.

tioned in front of a suitably shaped (flat helical) superconducting coil coupled to a SQUID in the circuit shown in Fig. 5.

The coil carries a persistent current I_0 . The diaphragm displacement x induces a change αx in the inductance L of the coil. Because of flux conservation, this motion causes a change in the currents circulating in the superconducting circuit, including a change $\delta\phi$ in the magnetic flux read by the SQUID. Circuit analysis applied to the circuit of Fig. 5 gives

$$\delta\phi = M I_0 \frac{\alpha x}{L} \frac{L_1}{L_1 + L_2 (1 + L_1/L)} \cong M I_0 \alpha x / L, \quad (\text{B1})$$

where in the approximated result we have assumed $L \cong L_1 \gg L_2$. To a first approximation, $\alpha/L = L^{-1} (dL/dx) \cong \xi/x_0$, with x_0 the equilibrium distance between the coil and diaphragm and ξ a factor of order unity.³⁴

A SQUID noise spectrum $\sqrt{S_\phi(\omega)}$ is usually flat, $\sqrt{S_\phi(\omega)} = \sqrt{S_\phi}$, in the frequency range where the oscillator is operated. This noise can be converted to a displacement noise S_x using Eq. (B1):

$$S_x = S_\phi \left\{ \frac{x_0}{M I_0 \xi} \right\}^2. \quad (\text{B2})$$

With typical values of $x_0 \approx 0.2$ mm, $I_0 \approx 0.1$ A, $M \approx 10$ nH, and $\sqrt{S_\phi} \approx 10^{-4} \phi_0 / \sqrt{\text{Hz}}$, one gets $\sqrt{S_x} \approx 4 \times 10^{-14}$ m/Hz assuming $\xi = 1$. This figure is reasonably close to what has been obtained in practice.^{28,35} Limiting sensitivities of better than 2×10^{-17} m/ $\sqrt{\text{Hz}}$ have been predicted for similar transducers.³⁴

As explained above, the ZAV oscillator is used to perform a measurement of the apparent critical mass current in the orifice. The mass current in the orifice, I_1 , is related to the diaphragm displacement (see Appendix A) by

$$I_1 = \frac{L_2}{L_1 + L_2} S \rho \frac{dx}{dt}. \quad (\text{B3})$$

Using Eqs. (B3) and (A12), one can convert the displacement noise into an equivalent angular velocity noise as

$$\sqrt{S_{\Omega d}} = L_2 (S \rho) (\frac{1}{2} \pi N R^2) (\omega_0 \sqrt{S_x}), \quad (\text{B4})$$

where ω_0 is the angular frequency of the oscillator.

Equation (B4) should be compared with the uncertainty due to the intrinsic noise mechanism arising from the stochastic nature of the phase-slip process:

$$\sqrt{S_{\Omega_i}} = (L_1 + L_2)(\rho\pi r^2)\Delta v_c(\frac{1}{2})\pi NR^2 / \sqrt{\omega_0/2\pi}. \quad (\text{B5})$$

These two contributions become equal if

$$\omega_0 = \{[(L_1 + L_2)/L_2](\rho\pi r^2/S)\Delta v_c / \sqrt{S_x/2\pi}\}^{2/3},$$

and this sets an upper limit to the frequency of operation of the oscillator. Taking $L_1 = L_2$, $s_1 = 8 \times 10^{-13} \text{ m}^2$, $S = 2 \times 10^{-4} \text{ m}^2$, $\sqrt{S_x} = 10^{-14} \text{ m}/\sqrt{\text{Hz}}$, and $\Delta v = 0.27 \text{ m/s}$, as predicted at 1 K from Eq. (12), one gets $\omega_0/2\pi \approx 1 \text{ kHz}$.

The SQUID will also contribute a back action force on the diaphragm. This force is due to thermal current noise³⁶ in the SQUID ring. The effect of this random force can be evaluated, and it is found to be of negligible importance for any realistic value of the system parameters.

- ¹M. Cerdonio and S. Vitale, Phys. Rev. B **29**, 481 (1984); Bonaldi *et al.*, in *Proceedings of the 4th Marcel Grossman Meeting on General Relativity*, edited by R. Ruffini (Elsevier, Amsterdam, 1986), p. 1309.
- ²M. Bonaldi, S. Vitale, and M. Cerdonio, Phys. Rev. B **42**, 9865 (1990).
- ³J. Anandan, Phys. Rev. Lett. **47**, 463 (1981); J. Anandan and R. Y. Chiao, Gen. Relativ. Gravit. **14**, 515 (1982).
- ⁴R. W. Guernsey, Jr., in *Proceedings of the 12th Conference on Low Temperature Physics*, edited by E. Kenda (Keigaku, Tokyo, 1971).
- ⁵J. C. Davis and R. E. Packard (unpublished).
- ⁶O. Avenel and E. Varoquaux, Jpn. J. Appl. Phys. **26**, 1798 (1987).
- ⁷T. A. Herring (unpublished). See also B.F. Chiao, EOS, Transactions of the AGU (to be published).
- ⁸L. D. Landau and E. M. Lifshitz, *The Classical Theory of Fields* (Addison-Wesley, Reading, MA 1951), p. 328.
- ⁹See, for instance, D. Vollhardt and P. Wölfle, *The Superfluid Phases of Helium 3* (Taylor & Francis, London, 1990).
- ¹⁰See, for instance, J. Wilks, *The Properties of Liquid and Solid Helium* (Clarendon, Oxford, 1967).
- ¹¹W. F. Vinen, Nature **181**, 1524 (1958); G. W. Rayfield and F. Reif, Phys. Rev. **136**, A1194 (1964); E. J. Yarmchuk and R. E. Packard, J. Low Temp. Phys. **46**, 4790 (1982).
- ¹²J. C. Davis, J. C. Close, R. J. Zieve, and R. E. Packard, Phys. Rev. Lett. **66**, 329 (1991).
- ¹³For the partitioned torus with arbitrary radii, the exact irrotational flow field can be found by conformal mapping techniques. In unpublished work (O. Alvarez and A. L. Fetter), the solution shows that the solid-body solution is always a very good approximation at some radial position.
- ¹⁴W. O. Hamilton, in *Near Zero: New Frontiers of Physics*, edited by J. D. Fairbank, B. S. Deaver, Jr., C. W. F. Everitt, and P. F. Michelson (Freeman, New York, 1988).
- ¹⁵P. M. Morse and H. Feshbach, *Methods of Theoretical Physics* (McGraw-Hill, New York, 1953), p. 1294.
- ¹⁶See, for example, the discussion in J. S. Langer and J. D. Reppy, in *Progress in Low Temperature Physics*, edited by C. J. Gorter (North-Holland, Amsterdam, 1970), Vol. 6.
- ¹⁷P. W. Anderson, Rev. Mod. Phys. **38**, 298 (1966).
- ¹⁸O. Avenel and E. Varoquaux, Phys. Rev. Lett. **55**, 2704 (1985).
- ¹⁹A. Amar, S. Sasaki, J. Davis, and R. E. Packard, Phys. Rev. Lett. **68**, 2624 (1992).
- ²⁰Throughout this paper we aim the discussion at detecting changes in rotation rather than absolute rotation. The SHEG can detect absolute rotation by reorienting the loop with respect to the rotation vector.
- ²¹E. Varoquaux, W. Zimmermann, Jr., and O. Avenel, in *Excitations in 2-Dimensional and 3-Dimensional Quantum Fluids*, edited by A. F. G. Wyatt and H. J. Lauter (Plenum, New York, 1991).
- ²²It should be mentioned that objects of size 1 m have not yet been cooled to 10 mK. However, gravity antennas of meter dimensions, weighing 10^3 kg , have been cooled below 100 mK [G. Pizzella (private communication)]. There is no technological reason preventing the refrigeration of large objects to millikelvin temperatures.
- ²³E. Varoquaux (private communication).
- ²⁴J. S. Brooks, B. B. Sabo, P. C. Shubert, and W. Zimmermann, Jr., Phys. Rev. B **19**, 4524 (1979).
- ²⁵S. Vitale, M. Cerdonio, and M. Bonaldi, Physica **178B**, 347 (1982).
- ²⁶O. Avenel and E. Varoquaux, Phys. Rev. Lett. **60**, 416 (1988).
- ²⁷B. P. Beecken and W. Zimmermann, Jr., Phys. Rev. B **35**, 1630 (1987).
- ²⁸A. Amar, Y. Sasaki, J. C. Davis, and R. E. Packard, Physica B **165 & 166**, 753 (1990).
- ²⁹J. Hook, Jpn. J. Appl. Phys. **26**, 159 (1987).
- ³⁰B. P. Beecken and W. Zimmermann, Jr., J. Vac. Sci. Technol. A **3**, 1839 (1985); P. Sudraud, P. Ballongue, E. Varoquaux, and O. Avenel, J. Appl. Phys. **62**, 2163 (1987); A. Amar (unpublished).
- ³¹If the critical currents of the two holes differ, the depth of the modulation pattern is diminished in a linear fashion. Also, if the current-phase relation is not quite sinusoidal, numerical calculations show that the modulation is also diminished. However, as long as the current-phase relation is nonlinear, single valued, and periodic in phase, the maximum current through the device continues to display the qualitative features inherent in Eq. (29).
- ³²J. M. Martinis and J. Clarke, J. Low Temp. Phys. **61**, 227 (1985).
- ³³D. E. McCumber, J. Appl. Phys. **39**, 3113 (1968).
- ³⁴H. J. Paik, J. Appl. Phys. **47**, 1168 (1976).
- ³⁵O. Avenel and E. Varoquaux, in *Proceedings of the ICEC 11*, edited by G. Klipping and I. Klipping (Butterworth, Guildford, 1987), p. 587.
- ³⁶J. M. Martinis and J. Clarke, J. Low Temp. Phys. **65**, 459 (1986).